EUROPHYSICS LETTERS 15 February 2003

Europhys. Lett., **61** (4), pp. 541–546 (2003)

Onset of charge localisation on coupling multipolar absorption modes in supported metal particles

R. Lazzari[1,2], I. Simonsen[1,3] and J. Jupille[1]

[1] *Laboratoire CNRS/Saint-Gobain "Surface du Verre et Interfaces" F-93303 Aubervilliers, France*

[2] *CEA Grenoble, DRFMC/SP2M/IRS - F-38054 Grenoble, France*

[3] *Department of Physics, The Norwegian University of Science and Technology N-7034 Trondheim, Norway*

(received 13 November 2001; accepted in final form 2 December 2002)

PACS. 78.20.Bh – Theory, models, and numerical simulation.
PACS. 61.46.+w – Nanoscale materials: clusters, nanoparticles, nanotubes, and nanocrystals.
PACS. 73.20.Mf – Collective excitations (including excitons, polarons, plasmons and other charge-density excitations).

Abstract. – An experimental evidence of the local enhancement of the electric field on supported metal nanoparticles is given in the case of a silver thin film growing on alumina, as studied *in situ* by surface differential reflectance. The dynamic charge localisation is driven by the inter-particle coupling of the multipolar plasmon absorption modes. Those modes and the associated polarisation charges are assigned via the modeling of the optical response.

Because of the symmetry breaking due to the substrate, the optical response of supported particles exhibits a specific behaviour with respect to clusters embedded in a host matrix [1–7]. In an unbounded medium, provided that the light wavelength is much larger than the particle diameter, trends in the interaction of spherical particles with an external field $\boldsymbol{E}_0$ can be accounted for, in the framework of the Mie theory [1], by replacing spheres by dipoles $\boldsymbol{p} = \epsilon\alpha\boldsymbol{E}_0$, with ϵ and α being the dielectric function of the medium and the polarisability of the particles, respectively. Altering the symmetry of the particles by either bringing them in contact with a substrate [2–4] or introducing truncations or both [5–7], is expected to span a non-negligible part of the adsorbed energy into multipolar modes which arise from heterogeneities of the field within the particles. (The "modes", a term used for simplicity, are in fact plasmon-polariton states [8].) This should occur even in the quasi-static limit, while it is only for larger particle sizes that multipolar modes are evidenced in the optical response of embedded clusters [8, 9]. We have previously shown that calculations must be performed at a multipolar order to describe the optical behaviour of supported metal particles and to accurately determine their morphology [6, 7], the dipolar theory [10] giving only trends [7, 11]. Nevertheless, despite their key role, the multipolar excitations arising from the symmetry breaking have never been experimentally evidenced for supported particles.

At small separation length, particle-particle coupling is also expected to excite multipolar modes [12–14]. In line with this, metallic films close to the percolation threshold show resonant behaviours such as anomalous transmittance and reflectance in the infrared range [15],

Surface Enhanced Raman Spectroscopy (SERS) [16] for adsorbed molecules and electromagnetic coupling of plasma oscillations. Arising among adjacent objects, those couplings drive giant enhancements of the local electric field which have been predicted theoretically [17] prior to being observed by means of near-field optical microscopy within subwavelength areas of a percolated gold film [18]. More generally, the details of optical response of particles in complex environments are used as a non-destructive probe of their geometry [9]. Of course, regarding the complexity of percolating films, it is not possible to unravel the multiple origins of the macroscopic optical response as it is expressed by means of the Fresnel coefficients. Therefore, a direct proof of the dynamic charge localisation by interactions among the multipolar plasmon oscillations in particles of subwavelength size is still lacking. In the present letter, advantage is taken of the previously demonstrated capability of the light to probe *in situ* a thin-film growth in vacuum conditions [6,7], to examine the behaviour of localised absorption modes during such growth, with a peculiar attention to the shifts in energy of the modes and their changes in intensity upon increasing the particle-particle coupling. Those modes are then identified by modeling the reflection coefficient of the interacting supported clusters.

The experiments consisted in evaporating silver from an effusion cell on a clean α-$Al_2O_3(0001)$ surface [19] in ultra-high vacuum conditions, while recording surface differential reflectance (SDR) spectra in the UV-visible range. The silver/alumina system has been chosen because it has several favourable characteristics. Silver is a test bed for optical studies of particles because its quasi-free plasma resonances are undamped by inter-band transitions and can be easily probed by common optical means. The broad gap of alumina insures that the optical spectra are free of features coming from the substrate. The silver/alumina interface is abrupt and, due to the poor wetting of alumina by silver, depositions operated at 570 K lead to three-dimensional silver clusters with low size dispersions and aspect ratios close to those expected at equilibrium, as checked by *ex situ* imaging techniques [20]. Since the sample is illuminated during the deposition by the UV-visible light emitted by a deuterium lamp, the reflected light at glacing incidence (45°) was analysed, in either *s*- or *p*-polarisation, by a grating spectrograph and recorded on a multichannel analyser [20]. The probed quantity was the so-called Surface Differential Reflectance (SDR)

$$\frac{\Delta R(\omega)}{R(\omega)} = \frac{R(\omega) - R_0(\omega)}{R_0(\omega)}\,, \tag{1}$$

where $R_0(\omega)$ stands for the bare substrate reflectivity and $R(\omega)$ for that of the metal-covered surface.

The recorded spectra in *p*-polarisation depicted in fig. 1 highlight the substrate-induced splitting of the Mie resonance. In the over-simplified dipolar picture, the low- and high-resonances are commonly assigned to parallel and perpendicular dipolar absorption modes [1], respectively. Once nucleated, particles start to grow without significant interactions. At that stage, the decrease in the surface/bulk ratio of the growing particles results in a redshift of the high-energy resonance as a function of the mean deposited thickness. This phenomenon [21] can be rationalized in terms of the decrease of the coupling of the $5s$ electrons with the $4d$ shell. Upon further growing of the particles, neighbouring interactions become increasingly important. In the quasi-static limit, these are accounted for by representing particles by dipoles. Dipolar modes perpendicular to the surface tend to create on each particle a depolarisation field which enhances the dipole oscillator strength. As a result, these modes are blueshifted. This explains the switch from blue to red of the shift of the high-energy resonance at high silver coverage (fig. 1 and ref. [22]). Instead, the depolarisation field associated with dipolar modes parallel to the substrate reduces the frequency of the mode, as in the case

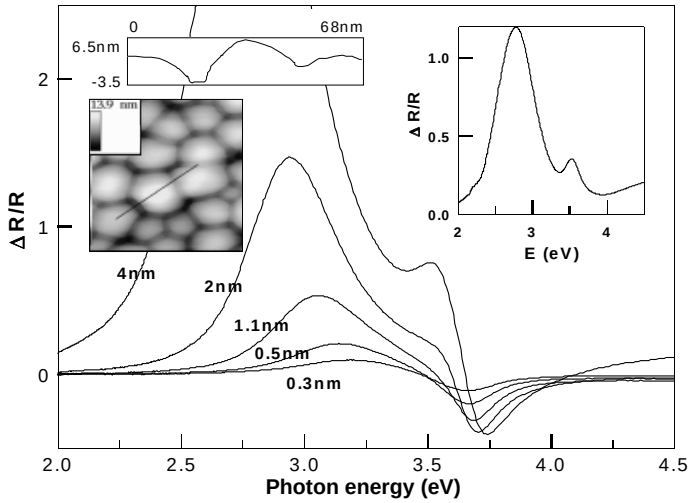

Fig. 1 – SDR spectra taken in p-polarisation (incident angle of 45°) for silver deposition on α-$Al_2O_3(0001)$ at 570 K, for average thicknesses ranging from 0.3 to 4 nm. The spectrum collected in s-polarisation in the same conditions for a thickness of 4 nm is displayed in the inset as well as a 100×100 nm AFM image of the final deposit.

of the low-energy resonance in fig. 1. Notably, the onset of the blueshift of the high-energy resonance coincides with the appearance of a shoulder in the spectra of fig. 1 which shows up around 3.5 eV. This shoulder is in better visibility in s-polarisation (inset of fig. 1), because the high-energy resonance mostly arises from normal components of the susceptibility (see below). As the silver coverage increases, it is slightly, but continuously, redshifted while its intensity increases. This and the strong redshift of the low-energy resonance make that feature more and more prominent in the SDR-spectra.

The optical spectra in both polarisations have been modeled by a previously described method [6, 7] based on the concepts of excess fields and surface susceptibilities [23], which has been shown to reproduce the experimental features to a large extent [6, 7, 20, 22] and to reasonably describe thin-film morphologies. For particles sizes (10 nm) much smaller than the light wavelength (200 to 800 nm), the cluster polarisability which mainly governs the electromagnetic far field behaviour of the film, *i.e.* its Fresnel coefficients [23], is calculated in the non-retarded limit. Clusters are modeled by truncated spheres. The Laplace equation is solved by an expansion into a series of spherical multipolar modes up to the M-th order [5, 6, 23]. The interaction with the substrate is represented via the introduction of image multipoles with respect to the surface. The polarisability of the individual islands is then renormalised by taking in account the interactions with the neighbouring particles up to dipolar order [24], a treatment which is valid up to a rather high coverage [25]. Finally, spectra have been fitted by accounting for the reduced mean-free path of s-electrons [1]. In the present case, a model was calculated for the spectrum collected after deposition of 4 nm of silver, as estimated by the quartz balance. A good fit including particle-particle interactions was found for a multipolar basis size of $M = 24$ where convergence was reached [6] (fig. 2). The obtained silver cluster density, diameter and aspect ratio (diameter/height) are $3.2 \cdot 10^{11}\,\mathrm{cm}^{-2}$, 12.8 nm and 1.27; a close agreement is found with *ex situ* AFM image (inset of fig. 1). The corresponding value of the average thickness, 2.8 nm, is consistent with a sticking coefficient lower than unity for Ag/α-$Al_2O_3(0001)$ [26]. To highlight how requisite is the introduction in calculations of both multipolar coupling with the substrate and lateral interactions, model spectra have been

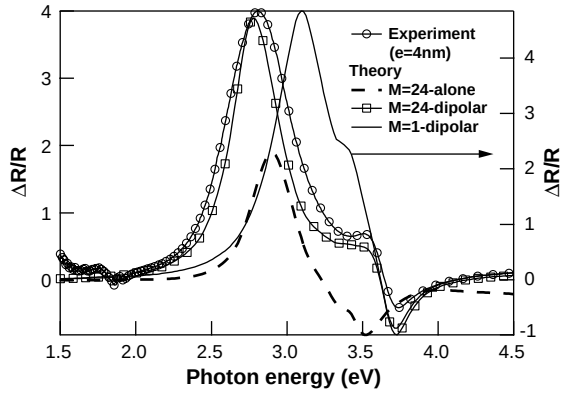

Fig. 2 – Modelling of the optical $\Delta R/R$ response of the 4 nm thick film: experimental spectrum (circles); model at an order $M = 24$ of multipolar expansion, without (dashed line) and with (squares) particle-particle dipolar coupling; model at an order $M = 1$ (continuous line).

calculated with the above-defined cluster morphology, i) without inter-particles coupling after calculation at the $M = 24$th order and ii) with inter-particles coupling, but at the order $M = 1$. Those models poorly compare to experiment (fig. 2). In addition, all attempts to get better fits in these two cases led to unacceptable values for the film morphology. Apart from a shift in energy of the low- and high-energy resonances, the main consequence of the introduction, within the $M = 24$ model, of the electromagnetic coupling between clusters is to nicely fit the feature lying around 3.5 eV (fig. 2). Beyond the confirmation of the above suggestion that the 3.5 eV feature is shifted in energy and enhanced in intensity by the lateral coupling between particles, this demonstrates that this feature involves multipolar resonances although these are not identified yet.

Widths of resonances are dictated by the imaginary part ϵ_i^{Ag} of the dielectric function of silver, while the positions in energy and the oscillator strengths are related to the real part ϵ_r^{Ag}. It can be anticipated that a simulated drastic decrease in the ϵ_i^{Ag} modulus should reveal each contributing resonance by narrowing its lineshape with no change in its energy position. In fig. 3a, reflectivity curves are calculated with a ϵ_i^{Ag} modulus artificially decreased to one per cent of its actual value, other things being equal with respect to fig. 2, either without (continuous line) or with (dotted line) lateral interactions. Optical activities with respect to the exciting field parallel (x) and normal (z) to the surface are indicated at the bottom of the figure. Since the integrated intensities of the calculated peaks shown in fig. 3a are expected to be indicative of the oscillator strengths of the modes, the three components labelled 1, 2, 3 in fig. 3a are likely to dominate the real spectrum. These features which are associated with the eigenmodes of the charge polarisation can be disclosed by mapping the potential within a symmetry plane which includes the exciting incident field (parallel or normal to the surface) (fig. 3b) [22]. The two major features 1 and 2 arise from polarisation charge distributions that can be described by dipoles parallel and perpendicular to the surface, respectively. The second-order mode 3 originates from a quadrupole pattern with an enhanced dipolar charge localisation on the cluster side. The other modes, not shown here, exhibit more complex behaviour. By defining interaction functions $I_\perp$ and $I_\parallel$ [5, 24], the perpendicular and parallel components of the polarisability on a given particle are renormalised by dipolar inter-particles interactions in the following way:

$$\alpha_\perp^I = \frac{\alpha_\perp}{1 - 2\alpha_\perp I_\perp} \quad \text{and} \quad \alpha_\parallel^I = \frac{\alpha_\parallel}{1 + \alpha_\parallel I_\parallel}\,. \tag{2}$$

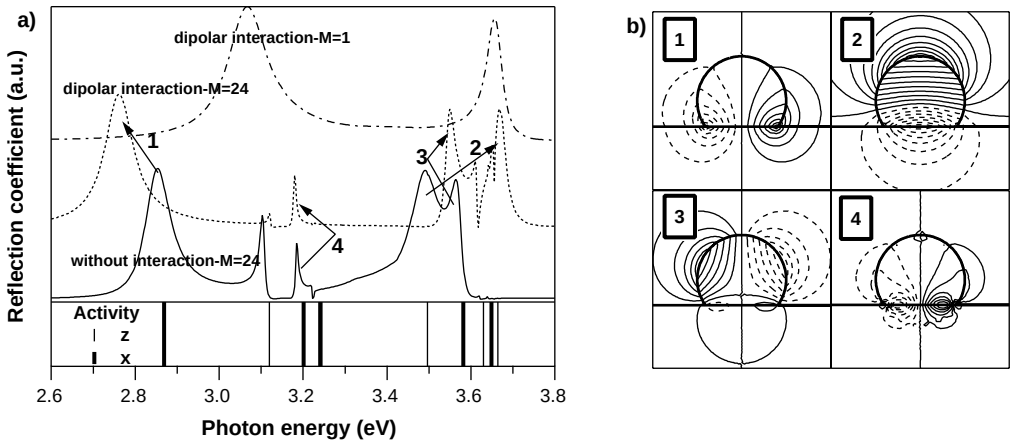

Fig. 3 – a) Modelling of the reflection coefficient in p-polarisation, corresponding to the 4 nm layer spectrum of fig. 1 after artificially lowering the imaginary part of the dielectric function (see text): i) at the order $M = 1$, without inter-particles coupling; ii) at the order $M = 24$ without and with coupling; the features of higher integrated intensities are labelled 1, 2, 3, 4; their shift upon introducing the coupling is shown by arrows; the x or z character of the modes (corresponding to $M = 24$ without coupling) is indicated at the bottom of the figure. b) Potential maps associated with the features 1, 2, 3, 4 showing, in the non-dissipative limit, the charge localisation on the silver cluster. The equipotential line scale which goes from negative (dashed line) to positive value (full line) is adapted to the mode oscillator strength.

Since the polarisability is in terms of a sum of Lorentz oscillators in the small damping limit:

$$\alpha = \sum_r \frac{F_r}{\omega_r - \omega - i\gamma_r}\,, \tag{3}$$

the renormalised expression of the polarisability can be written in an identical spectral representation but with shifted eigenfrequencies:

$$\omega^I_{r,\perp} = \omega_{r,\perp} - 2I_\perp F_{r,\perp} \quad \text{and} \quad \omega^I_{r,\parallel} = \omega_{r,\parallel} + I_\parallel F_{r,\parallel}\,. \tag{4}$$

Since the interaction parameters have negative values, the x-active modes are redshifted and the z-active modes blueshifted, according to the mode oscillator strength F_r. In fig. 3a, these shifts appear between the model without interactions and the model with interactions. Features 1, 2 and 3 behave consistently with the charge distributions pictured in fig 3b. A final proof about the nature of the modes comes from reflectivity spectra recorded in s-polarisation (inset of fig. 1). In this geometry, all the z-active modes should cancel. Indeed, in the inset of fig. 1, the mode 2 is no longer active. The absorption mode labeled 3, which has been predicted in fig. 3a to lie in the vicinity of 3.5 eV, shows up as a well-defined peak. (This peak possibly involves the mode labeled 4, expected to appear below 3.4 eV.) [22]. Apart from the low-energy resonance, which arises from a unique dipolar vibration with a pinning of the field-induced charge at the contact line between the three media (mode 1 in fig. 3b), the other regions of the spectrum involve mixtures of modes. High-order modes are not intense enough to modify the trends in energy dictated by the major contributions, but they likely perturb the shape of the spectra. An example is given by the energy range corresponding to modes 3 and 4. Particle-particle coupling manifests itself by both shifts in energy and increases in intensity of these modes so that at a fixed energy, say around 3.5 eV, the evolution of the morphology of the deposit during the growth induces a dynamic localisation of the charge and an enhancement

of the electric field around the cluster side (fig. 3b). In addition, one understands why, in a disordered system, mode couplings can induce hot spots for the electromagnetic field. The onset of local field enhancement is associated with the inter-particle coupling of the multipolar plasmon resonances, as it consistently arises within near-percolating film [18].

The *in situ* examination of the reflectance spectra of a silver thin film provided straightforward experimental evidences about the existence of spectral features associated with multipolar charge vibrations. These are brought about within the particles, even in the quasi-static limit, by the break in symmetry arising from both the contact with the substrate and the truncation of the particle. They show up upon the increase in the particle-particle coupling which simply results from the growth of the film. Their nature is disclosed by a modeling which demonstrates that most regions of the optical spectrum involve mixtures of modes. As an important consequence of the existence of these multipolar modes, the common picture of the optical response of supported metal particles, via simple dipole excitations by the parallel and normal components of the electric field, appears questionable.

REFERENCES

[1] Kreibig U. and Vollmer M., *Optical Properties of Metal Clusters*, Vol. **25** (Springer Verlag, Berlin) 1995.
[2] Johnson B., *J. Opt. Soc. Am.*, **13** (1996) 326.
[3] Beita C. *et al.*, *Phys. Rev. B*, **60** (1999) 6018; Román-Velázquez C. *et al.*, *Phys. Rev. B*, **61** (2000) 10427.
[4] Ruppin R., *Phys. Rev. B*, **45** (1992) 11209; 8.
[5] Wind M. and Vlieger J., *Physica A*, **141** (1987) 33; **143** (1987) 164.
[6] Simonsen I. *et al.*, *Phys. Rev. B*, **61** (2000) 7722.
[7] Lazzari R. *et al.*, *Eur. Phys. J. B*, **24** (2001) 267.
[8] Kreibig U. *et al.*, *Phys. Rev. B*, **36** (1987) 5027.
[9] Jin R. *et al.*, *Science*, **294** (2001) 1901.
[10] Yamaguchi T. *et al.*, *Thin Solid Films*, **18** (1973) 63; **21** (1974) 173.
[11] Martin D. *et al.*, *Surf. Sci.*, **377-379** (1997) 985.
[12] Claro F. and Rojas J., *Phys. Rev. B*, **34** (1986) 3730.
[13] Lebedev A. *et al.*, *J. Opt. A*, **1** (1999) 573.
[14] Hilger A. *et al.*, *Appl. Phys. B*, **73** (2001) 361.
[15] Cohen R. *et al.*, *Phys. Rev. B*, **8** (1973) 3689.
[16] Wang D. and Kerker M., *Phys. Rev. B*, **24** (1981) 1777.
[17] Shalaev V., *Phys. Rep.*, **272** (1996) 61.
[18] Grésillon S. *et al.*, *Phys. Rev. Lett.*, **82** (1999) 4520.
[19] Coustet V. and Jupille J., *Surf. Sci.*, **307-309** (1994) 1161.
[20] Lazzari R. *et al.*, *Appl. Surf. Sci.*, **142** (1999) 451.
[21] Liebsch A., *Phys. Rev. B*, **48** (1993) 11317; Feibelman P., *Surf. Sci.*, **282** (1993) 129.
[22] Lazzari *et al.*, *Phys. Rev. B*, **65** (2002) 235424.
[23] Bedeaux D. and Vlieger J., *Optical Properties of Surfaces* (Imperial College Press, London) 2001; *Physica A*, **67** (1973) 55; **73** (1973) 287; **82** (1976) 221.
[24] Vlieger J. and Bedeaux D., *Thin Solid Films*, **69** (1980) 107; **102** (1983) 265.
[25] Haarmans M. and Bedeaux D., *Thin Solid Films*, **224** (1993) 117.
[26] Van Campen D. and Hrbek J., *J. Phys. Chem. B*, **99** (1995) 16389.